JOURNAL OF MATERIALS SCIENCE 30 (1995) 5995–5998

Phase transformation of inviscid melt spun (IMS) alumina–zirconia eutectic fibres

YUN-MO SUNG*
Department of Materials Engineering, Rensselaer Polytechnic Institute, Troy, New York 12180, USA
S.A. DUNN‡ AND J.A. KOUTSKY‡§
‡Department of Chemical Engineering and §Materials Science Program, University of Wisconsin, Madison, Wisconsin 53706, USA

Al_2O_3–ZrO_2 (AZ) eutectic fibres containing 41.05 wt% ZrO_2 and 2.03 wt% Y_2O_3 were produced via inviscid melt spinning (IMS). Scanning electron microscopy (SEM) was used to examine the morphology of the as-spun AZ fibre. Differential thermal analysis (DTA) and X-ray diffraction (XRD) were used to investigate the phase transformations in this fibre. The XRD pattern of the as-spun AZ fibre showed tetragonal ZrO_2, α-Al_2O_3, and non-equilibrium δ-Al_2O_3 phase formation. The DTA curve of the as-spun AZ fibre showed only one endothermic peak representing the phase transformation of δ-Al_2O_3 to α-Al_2O_3. This phase transformation was confirmed by analysing the XRD pattern of heat-treated AZ fibre.

1. Introduction

The current ceramic fibre fabrication mainly depends on following methods: (1) chemical vapour deposition (CVD) of ceramics on tungsten or graphite filaments [1–4], (2) pyrolysis of cured polymer fibres [5–7], (3) slurry processing of ceramic powders and organic polymer mixture [8–10], and (4) diffusion-based sol–gel processing of metal alkoxides [11–13]. These techniques, however, are costly due to the slow speed of the processes. It is obvious that melt spinning is a much faster and low-cost fibre processing method, compared to the above techniques. Rayleigh break-up, however, is a crucial problem in spinning of inviscid melts of ceramic and metal. Inviscid melt spinning (IMS) is a noble process which can be applied to fibre production using low-viscosity melts [14–19]. The formation of a stabilizing sheath on the surface of inviscid molten stream by introduction of a reactive gas such as propane, can prevent the Rayleigh break-up and stabilize the molten stream until solidification occurs.

The first ceramic fibre spun by this IMS process was CaO–Al_2O_3 (CA) fibre produced by Cunningham *et al.* [14]. The crystallinity of this IMS CA fibre was intensively examined by Wallenberger and co-workers [20–22]. They found that the CA fibres were vitreous up to 82 wt% of Al_2O_3 as produced. Sung *et al.* [23, 24] found a non-equilibrium phase of $CaO\cdot Al_2O_3$ and equilibrium phases of $MgO\cdot Al_2O_3$ and α-Al_2O_3 in as-spun CaO–Al_2O_3–MgO (21 wt% CaO–74 wt% Al_2O_3–5 wt% MgO) IMS fibres. They heat treated this fibre at 1100 °C for 24 h and obtained equilibrium phases of $3CaO\cdot 5Al_2O_3$, $MgO\cdot Al_2O_3$, and α-Al_2O_3. Wallenberger *et al.* [21] also produced Al_2O_3–ZrO_2 (65.5 wt% Al_2O_3–34.2 wt% ZrO_2–0.3 wt% CaO) fibres by IMS. Their X-ray diffraction (XRD) patterns of this fibre unexpectedly showed formation of an only stabilized tetragonal ZrO_2 (t-ZrO_2) phase.

The eutectic Al_2O_3–ZrO_2 (AZ) fibres of 41.05 wt% ZrO_2 containing 2.03 wt% Y_2O_3 were produced to obtain high strength and high toughness reinforcements for composites. The purpose of this study is to investigate the morphology of the IMS AZ fibre using scanning electron microscopy (SEM) and identify the phase transformations in this fibre using XRD and differential thermal analysis (DTA).

2. Experimental procedure

The unique IMS apparatus mainly consists of three parts: (1) an induction heating unit, (2) a graphite crucible with orifice at the bottom and associated gas plate assembly, and (3) three containment chambers. Fig. 1 shows a schematic diagram of the IMS unit [25].

High purity Al_2O_3, ZrO_2, and Y_2O_3 powders were well mixed using zirconia ball-milling (YTZ Zirconia-Ball Media, Tosoh USA Inc., Atlanta, GA, USA). The mixed powders (~ 100 g) were loaded inside the graphite crucible and heated in a vacuum atmosphere (~ 6.6×10^{-5} atm) by induction heating (maximum capacity of 15 kW and 10 kHz). Before melting the powders at 1910 °C, both the furnace and intermediate

---

*Author to whom all correspondence should be addressed.

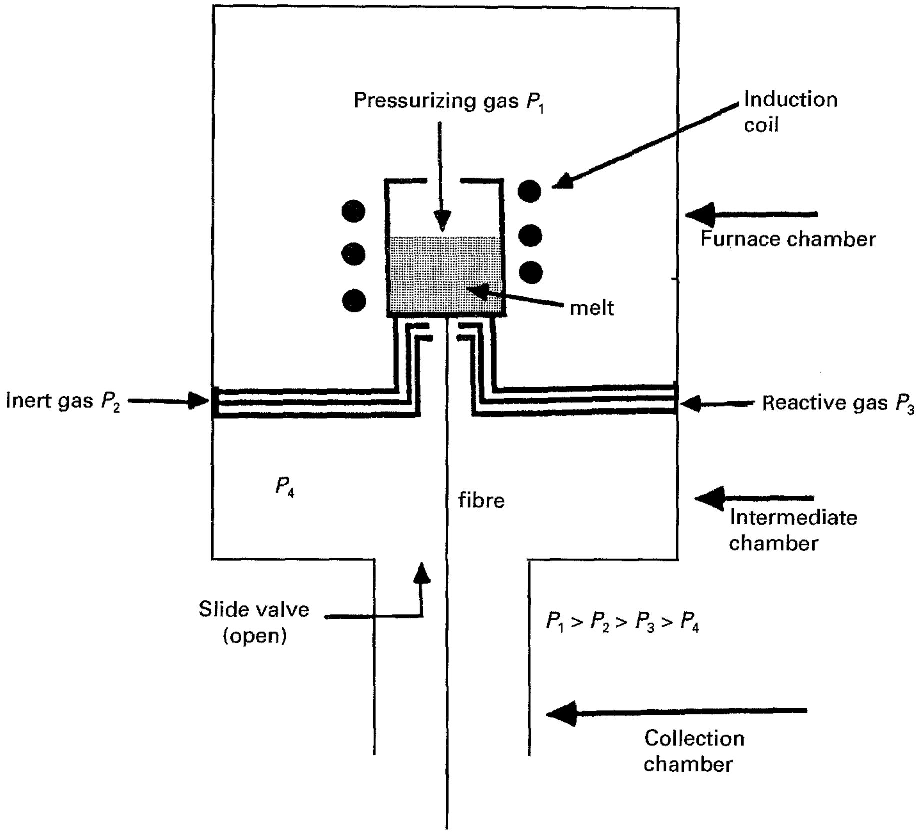

Figure 1 The schematic diagram of inviscid melt spinning (IMS) unit [25].

TABLE I Phase identification of inviscid melt spun (IMS) Al_2O_3–ZrO_2 eutectic fibre

d-spacings (nm) (2θ (deg.))	Crystalline phases		
	t-ZrO_2	δ-Al_2O_3	α-Al_2O_3
$d_1(2\theta)_1$	0.296 (30.17)	0.1396 (66.97)	0.2085 (43.36)
$d_2(2\theta)_2$	0.183 (49.78)	0.1986 (45.64)	0.2552 (35.13)
$d_3(2\theta)_3$	0.1547 (59.72)	0.2460 (36.49)	0.1601 (57.66)
$d_4(2\theta)_4$	0.181 (50.37)	0.1407 (66.38)	0.3479 (25.64)
$d_5(2\theta)_5$	0.1575 (58.56)	0.2279 (39.51)	0.1374 (68.19)
	0.254(35.31)	0.1953 (46.46)	
$d_6(2\theta)_6$	0.260 (34.47)	0.2728 (32.14)	0.2379 (37.78)
$d_7(2\theta)_7$	0.1493 (62.12)	0.2601 (34.45)	0.1740 (52.55)
	0.190 (80.67)		

chambers were filled with argon gas at a pressure of ~ 50 psi to prevent violent gas evolution from the melt. To homogenize the melt, the temperature was held at 1950 °C for 20 min. When the slide valve between the intermediate and catch chambers was opened the intermediate chamber quickly dropped to atmospheric pressure. The pressure difference between the furnace chamber and the intermediate chamber extruded the molten AZ through the orifice and into the intermediate chamber atmosphere. Once the molten stream was continuously flowing as droplets, the reactive gas (propane) was introduced through the gas plates. The carbon deposition on the molten stream results from pyrolysis of propane gas by the heat from the molten stream as following:

$$C_3H_8(g) \xrightarrow{\text{heat}} 3C(s) + 4H_2(g) \qquad (1)$$

The microstructure of the as-spun AZ fibre was examined using SEM (Jeol SEM 35-C, Japan). To identify the crystalline phase in the as-spun AZ fibres, powdered AZ fibres were investigated using an XRD (Nicolet Stoe Transmission/Bragg-Brentano, Stoe Co., Germany) with a CuK_α source, 15 s time constant, 20 to 70° scan range, and 0.02° step size. The resulting XRD patterns were identified using the Joint Committee on Powder Diffraction Standards (JCPDS) cards. DTA (Perkin-Elmer DTA 1700, Norwalk, CT, USA) was performed to investigate the phase transformations of this fibre. AZ fibres ($\approx$ 1 cm long and total weight of 100 mg) were loaded inside a platinum crucible and heated from 25 to 1400 °C at a heating rate of 10 °C min^{-1} in an air atmosphere. DTA temperatures were calibrated using pure Al and Cu. As-spun AZ fibres were heated from 25 to 1280 °C at a heating rate of 10 °C min^{-1} inside a horizontal furnace (DT-31-HT, Deltech Inc., Denver, CO, USA) in an air atmosphere and then quenched in water. The heat-treated AZ fibres were ground and phase analysed by XRD. Table I shows a list of XRD peak positions of tetragonal ZrO_2, δ-Al_2O_3, and α-Al_2O_3 in decreasing order of intensities, as given in the JCPDS cards.

3. Results and discussion

During IMS the AZ molten streams became partially stabilized within a few seconds or less. Thermodynamic stability of a mixture of molten Al_2O_3 and ZrO_2 against reduction by carbon at 1950 °C was examined

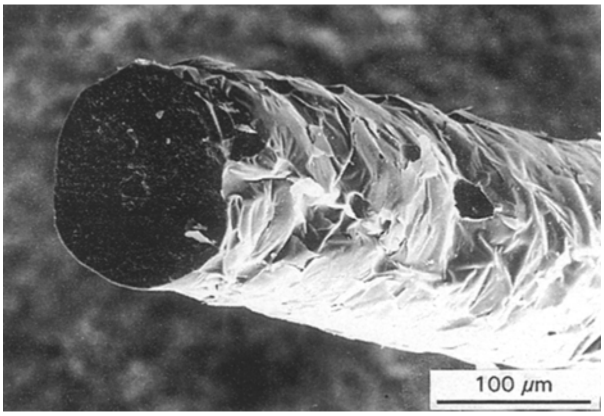

Figure 2 The scanning electron micrograph (SEM) of as-spun Al_2O_3–ZrO_2 eutectic fibre produced by inviscid melt spinning (IMS).

by the following:

$$Al_2O_3(l) + 3C(s) \rightarrow 2Al(l) + 3CO(g)$$

$$\Delta G^\circ = +45.00\ \mathrm{kJ\,mol^{-1}}\ \text{at}\ 1950^\circ\mathrm{C} \quad (2)$$

$$ZrO_2(l) + 2C(s) \rightarrow Zr(l) + 2CO(g)$$

$$\Delta G^\circ = +64.71\ \mathrm{kJ\,mol^{-1}}\ \text{at}\ 1950^\circ\mathrm{C} \quad (3)$$

These positive free energy values imply that neither Al_2O_3 nor ZrO_2 will be reduced to Al or Zr at 1950 °C.

Approximately 130 μm diameter and 6 cm long fibres were produced with fine droplets. Most of the AZ fibres were slightly curly in shape. The surface of the fibres was black. Obvious surface roughness indicating crystallinity was observed in SEM of the as-spun AZ fibre as shown in Fig. 2. Porosity inside the fibre would most likely come from shrinkage during solidification and porosity at the surface of the fibre would come from a possible gas evolution during cooling. The exact mechanism of the porosity formation is not clear at the present time. The porosities will degrade the mechanical properties of this AZ fibre. The mechanical properties of this AZ fibre are being investigated and will be published soon.

XRD was performed to examine crystalline phases in the AZ fibre. Fig. 3a shows XRD patterns of the as-spun AZ fibres. Identification of phases in the fibre can be accomplished through comparison of XRD peak locations and intensities with those of the standards in Table I. High intensity peaks from tetragonal ZrO_2 phase and low intensity peaks from δ-Al_2O_3 and α-Al_2O_3 are identified. This result is contradictory to the result of Wallenberger *et al.* [21], showing only t-ZrO_2 phase formation in 34.2 wt % ZrO_2 fibre which somehow should show an Al_2O_3 phase. The peak positions in terms of *d*-spacing for t-ZrO_2, listed in decreasing order of intensity, are 0.296, 0.182, 0.254, 0.180, 0.154, 0.259, and 0.156 nm. The peak positions are in good agreement with those in Table I, whereas the order of intensities are not. The peak at 0.254 nm shows the overlapping of two peaks from t-ZrO_2 and α-Al_2O_3. The peak positions for δ-Al_2O_3, listed in decreasing order of intensity, are 0.139, 0.245, 0.198, 0.141, 0.195, 0.273, and 0.227 nm. This result corresponds well to the data in Table I. The peak positions for α-Al_2O_3, listed in decreasing order of intensity, are 0.254, 0.208, 0.160, 0.348, 0.138, 0.174, and 0.238 nm. All of the peak positions agree well with the data in Table I.

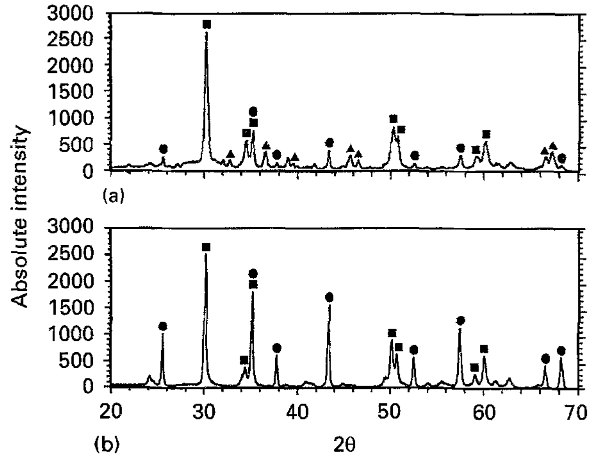

Figure 3 The X-ray diffraction (XRD) pattern of as-spun Al_2O_3–ZrO_2 eutectic fibre which is showing crystalline phase formation of t-ZrO_2, (■), δ-Al_2O_3 (▲), and α-Al_2O_3 (●) (a), and the XRD pattern of Al_2O_3–ZrO_2 eutectic fibre heat-treated from 25 to 1280 °C at heating rate of 10 °C min^{-1} and water-quenched at 1280 °C which is showing crystalline phase formation of t-ZrO_2 (■) and α-Al_2O_3 (●) (b).

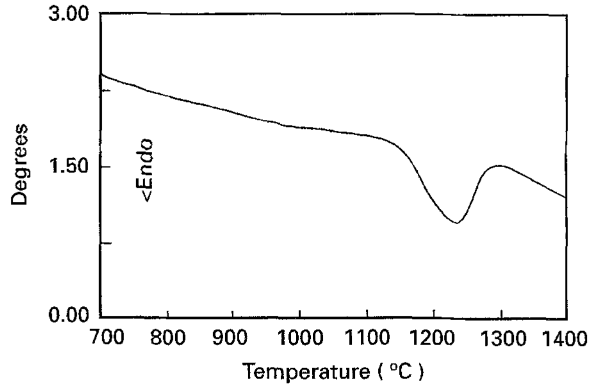

Figure 4 The differential thermal analysis curve of as-spun Al_2O_3–ZrO_2 fibre at heating rate of 10 °C min^{-1}.

To investigate possible phase transformation in this as-spun AZ fibre, DTA was performed. The DTA curve in Fig. 4 shows one endothermic peak ranging from 1160 to 1280 °C at a heating rate of 10 °C min^{-1}. The peak temperature was 1235 °C. Any exothermic peak representing crystallization of the amorphous phase in the as-spun AZ fibre was not detected from this DTA curve. This implies that the AZ fibres are fully crystallized as prepared.

To identify the phase transformation, the as-spun AZ fibres were heated from 25 to 1280 °C at a heating rate of 10 °C min^{-1} inside a furnace and quenched into water at 1280 °C. The heat-treated AZ fibres were ground and phase analysed using XRD. Obviously, the peak intensities of α-Al_2O_3 increased and δ-Al_2O_3 peaks disappeared as shown in Fig. 3b. Therefore, it can be concluded that the endothermic peak in the DTA curve corresponds to the phase transformation of δ-Al_2O_3 to α-Al_2O_3. The peak positions and intensities of t-ZrO_2 phase remain approximately the same as in Fig. 3a.

4. Conclusions

SEM of IMS Al_2O_3–ZrO_2 (AZ) fibre showed surface roughness due to crystallinity and some porosities possibly due to shrinkage and gas evolution during solidification. XRD patterns of the as-spun IMS AZ fibre showed formation of equilibrium t-ZrO_2, α-Al_2O_3 phases, and a non-equilibrium δ-Al_2O_3 phase. DTA result of the AZ fibre showed a phase transformation ranging from 1160 to 1280 °C. This was identified as the phase transformation of δ-Al_2O_3 to α-Al_2O_3 from the XRD result of the AZ fibre which was heated up to 1280 °C and then quenched.

Acknowledgement

The authors wish to thank Mr Sungtae Kim at University of Wisconsin-Madison for kindly providing access to DTA.

References

1. J. O. CARLSSON, in "Encyclopedia of materials science and engineering" edited by M. B. Bever (Pergamon Press, Oxford, 1986) p. 4406.
2. P. MARTINEAN, M. LAHAYE, R. PAILLER, R. NALSAN, M. COUZI and F. CRUEGE, *J. Mater. Sci.* **19** (1984) 2371.
3. S. R. NUTT and F. E. WAWNER, *ibid.* **20** (1985) 1953.
4. J. A. DICARLO, *ibid.* **21** (1986) 217.
5. S. YAJIMA, Y. HASEGAWA, J. HAYASI and M. IMURA, *ibid.* **13** (1978) 2569.
6. Y. HASEGAWA, *ibid.* **24** (1989) 1177.
7. K. OKAMURA, M. SATO, T. MATSUZAWA, T. SEGUCHI and S. KAWANISHI, *Ceramic Eng. Sci. Proc.* **9** (1988) 909.
8. J. D. BIRCHALL, in "Encyclopedia of materials science and engineering" edited by M. B. Bever (Pergamon Press, Oxford, 1986) p. 2333.
9. J. D. BIRCHALL, J. A. BRADBURY and J. DINWOODIE, in "Handbook of composites" edited by W. Watt and B. V. Perov (Amsterdam, North-Holland).
10. S. NOURBAKHSH, F. L. LIANG and H. MARGOLIN, *J. Mater. Sci. Lett.* **8** (1989) 1252.
11. K. R. VENKATACHARI, L. T. MOETI, M. D. SACKS and J. H. SIMMONS, *Ceram. Eng. Sci. Proc.* **11** (1990) 1512.
12. D. D. JOHNSON, A. R. HOLTZ and M. F. GRETHER, *ibid.* **8** (1987) 744.
13. T. NISHIO and Y. FUJIKA, *J. Ceram. Soc. Jpn. Int.* **99** (1991) 638.
14. R. E. CUNNINGHAM, L. F. RAKESTRAW and S. A. DUNN, in "Spinning Wire From Molten Metal" AIChE Symposium Series, Vol. **74**, edited by J. W. Mottern and W. J. Privott (American Institute of Chemical Engineers, New York 1978) p. 20.
15. B. S. MITCHELL, K. Y. YON, S. A. DUNN and J. A. KOUTSKY, *Mater. Lett.* **10** (1990) 71.
16. F. T. WALLENBERGER, N. E. WESTON and S. A. DUNN, *J. Non-Cryst. Sol.* **24** (1990) 116.
17. F. T. WALLENBERGER, N. E. WESTON and S. A. DUNN, *SAMPE Quart.* **9** (1990) 121.
18. F. T. WALLENBERGER, *Ceram. Bull.* **69** (1990) 1646.
19. B. S. MITCHELL, K. Y. YON, S. A. DUNN and J. A. KOUTSKY, *Chem. Eng. Comm.* **106** (1991) 87.
20. F. T. WALLENBERGER, N. E. WESTON, K. MOTZFELT and D. G. SWARTZFAGER, *J. Amer. Ceram. Soc.* **75** (1992) 629.
21. F. T. WALLENBERGER, N. E. WESTON and S. A. DUNN, *J. Mater. Res.* **5** (1990) 2682.
22. F. T. WALLENBERGER, N. E. WESTON and S. A. DUNN, *SAMPE Quart.* **21** (1990) 30.
23. Y.-M. SUNG, S. A. DUNN and J. A. KOUTSKY, *Ceram. Int.* **20** (1994) 337.
24. Y.-M. SUNG, PhD thesis, University of Wisconsin-Madison (1994).
25. B. S. MITCHELL, PhD thesis, University of Wisconsin-Madison (1991).

Received 27 January
and accepted 24 May 1995